ELSEVIER

Biochimica et Biophysica Acta 1463 (2000) 307–322

BIOCHIMICA ET BIOPHYSICA ACTA

BBA

www.elsevier.com/locate/bba

Cardiolipin, α-D-glucopyranosyl, and L-lysylcardiolipin from Gram-positive bacteria: FAB MS, monofilm and X-ray powder diffraction studies

T. Gutberlet [a,b,*], U. Dietrich [b], H. Bradaczek [a], G. Pohlentz [c], K. Leopold [d], W. Fischer [d,1]

[a] *Institut für Kristallographie, Takustr. 6, D-14195 Berlin, Germany*
[b] *Institut für Experimentelle Physik I, Linnestr. 5, D-04103 Leipzig, Germany*
[c] *Institut für Physiologische Chemie, Nussallee 11, D-53115 Bonn, Germany*
[d] *Institut für Biochemie, Medizinische Fakultät, Fahrstr. 17, D-91053 Erlangen, Germany*

Received 14 July 1999; received in revised form 12 October 1999; accepted 25 October 1999

Abstract

Cardiolipin preparations from *Streptococcus* B, *Listeria welshimeri*, *Staphylococcus aureus*, and a glucosyl and lysyl derivative of cardiolipin were analysed for fatty acid composition and fatty acid combinations. Three different fatty acid patterns are described and up to 17 molecular species were identified in *Streptococcus* B lipids by high resolution FAB MS. The physicochemical properties of these lipids were characterised in the sodium salt form by monofilm experiments and X-ray powder diffraction. All lipids formed stable monofilms. The minimal space requirement of unsubstituted cardiolipin was dictated by the fatty acid pattern. Substitution with L-lysine led to a decrease of the molecular area, substitution with D-glucopyranosyl to an increase. On self assembly at 100% relative humidity, all preparations adopted lamellar structures. They showed a high degree of order, in spite of the heterogeneous fatty acid compositions and numerous fatty acid combinations. The repeat distances in lamellar fluid phase varied between 4.99 and 5.52 nm, the bilayer thickness between 3.70 and 4.46 nm. Surprising were the low values of sorbed water per molecule of the glucosyl and lysyl derivatives which were 58 and 60%, compared with those of the respective cardiolipin. When Na^+ was replaced as counterion by Ba^{2+}, the bilayer structure was retained, but the lipids were in the lamellar gel phase and the fatty acids were tilted between 32 and 53° away from the bilayer normal. Wide angle X-ray diffraction studies and electron density profiles are also reported. Particular properties of glucosyl cardiolipin are discussed.

Keywords: Cardiolipin; Fatty acid pattern; Fatty acid combination; D-Glucosylcardiolipin; L-Lysylcardiolipin; Fast atom bombardment mass spectroscopy; Monofilm; X-ray powder diffraction

Abbreviations: POPC, 1-palmitoyl-2-oleoyl-*sn*-glycero-3-phosphocholine; FAB MS, fast atom bombardment mass spectroscopy; Lα, lamellar fluid phase; Lβ, lamellar gel phase; H_{II}, inverted hexagonal phase; *d*, symbol for repeat distance; l, symbol for lipid

* Corresponding author. Present address: Hahn–Meitner-Institut Berlin GmbH, Department NE, Glienicker Str. 100, D-14109 Berlin, Germany. Fax: +49-30-8062-2999; E-mail: gutberlet@hmi.de

[1] E-mail: w.fischer@biochem.uni-erlangen.de

0005-2736/00/$ – see front matter
PII: S0005-2736(99)00214-X

1. Introduction

Cardiolipin (bisphosphatidylglycerol), an anionic teraacylphospholipid, is in the eucaryotic cell almost exclusively confined to the inner mitochondrial membrane [1,2] and occurs in the cytoplasmic membrane of Gram-positive and Gram-negative bacteria [2–4]. The concentration in the membrane of Gram-positive bacteria varies from a few mole percent during exponential growth in *Staphylococcus aureus* [5] to 59 mol% in streptococci [2]. It increases in *S. aureus* at the cost of phosphatidylglycerol under the conditions of ATP deprivation [5], postexponential growth [6], growth on high salt concentration [7], and autoplast formation [8]. Since the backbone glycerol of cardiolipin is more rigid than the headgroups of other phospholipids [9], the conversion of phosphatidylglycerol to cardiolipin under the aforementioned conditions may increase the order and presumably the stability of the membrane.

Due to the relative small headgroup in comparison to the total hydrocarbon chain volume, cardiolipin is particularly prone to polymorphic phase behaviour. Although the lamellar arrangement is thought to predominate in biological membranes, the inverted hexagonal H_{II} structure can in vitro be readily induced by addition of divalent cations [10], by pH titration or by increasing the monovalent ion concentration [11,12].

Intramolecular hydrogen bonds between the hydroxy group of the glycerol unit and the oxygen at the neighbouring phosphate groups have been reported [13,14]. The authors discussed the possibility that these hydrogen bonds might be involved in the migration of protons along the membrane surface which is the central part of the 'localised' theory of energy transfer between proton pumping by the respiratory chain and proton utilisation by ATPase [15–18]. Alterations of cardiolipin at the hydroxy group of the glycerol unit should change the biophysical and structural properties of the molecule, i.e. suppression of intramolecular hydrogen bonding and alterations of the polymorphisms. Actually, the synthetic 2′-deoxy analogue lost the ability of intramolecular hydrogen bonding [13,14] and semisynthetic acylcardiolipin spontaneously adopted the hexagonal phase with the additional fatty acid preventing the conversion to the lamellar phase [12].

Except α-D-glucopyranosylcardiolipin, naturally occurring substituted cardiolipins have not been reported. It is noteworthy that glucosylcardiolipin was found in the four strains of group B streptococci studied [19]. It amounts to 8 mol% of membrane lipids and contributes 19% to the lipid phosphorus. Recently discovered representatives of this new lipid class are D-alanylcardiolipin [20] and L-lysylcardiolipin [21]. D-Alanylcardiolipin is a characteristic membrane lipid of *Vagococcus fluvialis* where it contributes 11 and 26 mol% to exponential and stationary growth phase membrane lipids [20]. L-Lysylcardiolipin was discovered in the four *Listeria* species tested [21]. Along with cardiolipin it is a typical late exponential growth phase lipid and contributes at this stage more than 40% to the membrane lipid phosphorus.

In this communication, we report on FAB MS, monofilm and X-ray powder diffraction studies of α-D-glucopyranosyl- and L-lysylcardiolipin isolated from group B *Streptococcus* and *Listeria welshimeri*, respectively. The unsubstituted cardiolipins of the same bacteria and the cardiolipin of *S. aureus* were included in order to evaluate the influence of the substituents on the physical properties. To the best of our knowledge, the physical properties of cardiolipin of Gram-positive bacteria have not been studied so far.

2. Materials and methods

2.1. Preparation of lipids

Total membrane lipids were extracted from group B *Streptococcus* Kiel 090 [19,22], *S. aureus* DSM 20233 [5,23] and *L. welshimeri* SLCC 5334^T [21]. Crude lipids were separated, individual lipids purified and structurally characterised as described in the references given. Molecular species of different fatty acid combinations were identified by negative ion FAB MS ([24] and this report). The molecular weight, given in Tables 1 and 2, are those of the predominant molecular species. Purified cardiolipins and their derivatives were first converted to the acid form by passing them in $CHCl_3$/MeOH (1:2, v/v) through small columns (Pasteur pipettes) of cation exchange resin, H^+, prewashed with the same solvent

mixture. Conversion into the sodium salt form was achieved by addition of one fourth volume of 0.2 M NaCl containing 10 mM $NaHCO_3$. The mixture was shaken vigorously (20 min) and then centrifuged for phase separation. The lower $CHCl_3$ layer was washed several times with quartz-distilled water. Barium salts were prepared in the same way, except that NaCl/$NaHCO_3$ was replaced by 0.1 M $BaCl_2$ containing 1 mM $Ba(OH)_2$.

2.2. FAB MS

The fast atom bombardment mass spectrometry (FAB MS) analyses were carried out on a VG-ZAB-T four sector instrument (Fisons Instruments, Manchester, UK). For atom bombardment cesium was used and the applied acceleration voltage was 8 kV. A mixture of thioglycerol (tgl) and M-nitrobenzylalcohol (mNBA) (1:1, v/v) was used as matrix. The samples were dissolved (5 mM) in chloroform/methanol (2:1, v/v) and 1 μl of a sample solution was added to the matrix. Negative ions (FAB(−)) were detected after the first electrostatic analyser on the second photomultiplier point detector. The spectra were run in a mass range from 100 to 2000 atom mass units (amu) with a scan rate of 8 s per decade and up to 20 scans were accumulated. For data acquisition and data processing the Opus V3.1X software was used.

2.3. Monofilm measurements

Cardiolipin of *S. aureus* was dissolved in chloroform/propanol (3.4:1, v/v), α-D-glucosyl-cardiolipin of *Streptococcus* B in chloroform/propanol (3:1, v/v). Cardiolipin and L-lysyl-cardiolipin of *L. welshimeri* and cardiolipin of *Streptococcus* B were dissolved in chloroform. All solvents used were of analytical grade (Merck, Darmstadt, Germany). Monofilms were prepared by spreading the lipid solution in organic solvent with a syringe on the aqueous subphase containing 0.01 M NaCl. The water used was tridistilled in a quartz apparatus. The areas of the monofilms were measured at a round trough [25] at 20°C on compression at a speed of 0.08–0.1 nm^2/min.

2.4. X-ray powder diffraction measurements

Small droplets of the solutions of cardiolipin of *S. aureus*, *Streptococcus* B and *L. welshimeri*, L-lysyl-cardiolipin of *L. welshimeri* and α-D-glucosylcardiolipin of *Streptococcus* B were placed on pieces of Si-wafers (Wacker Chemitronic, Burghausen, Germany) to cover an area of about 5×5 mm.

The samples were dried on air to give random numbers of lipid layers along the wafer surface. The dried samples were placed in a thermostated and sealed chamber mounted on a Philips X-ray powder diffractometer PW 3020 (Philips, Eindhoven, Netherlands), which was run with Ni-filtered Cu K_α radiation at 20 mA/30 kV. Measurements were done in the θ–2θ mode (Bragg–Brentano) with step width of 0.02° 2θ. The sampling time varied between 1 and 10 s per step. Scattered intensity was collected with a proportional counter.

Samples were first measured on air in the open chamber at 25°C at relative humidity of $60 \pm 3\%$. Then a small bowl with water was placed into the chamber, the chamber was sealed and the samples were rehydrated at 25°C at 100% relative humidity within 36 h and measured again.

Numbers of oriented multilayers of cardiolipin of *S. aureus* on solid supports (glass slides) were obtained by the Langmuir–Blodgett technique. Multilayers were placed on hydrophilic glass slides cleaned with ethanol by moving the glass slide vertically up and down through a monofilm at a speed of 6 mm/min. The monofilm was spread on an aqueous subphase and compressed to 36 mN/m. Up to 16 bilayers were transferred. The samples were dried on air, placed on the X-ray powder diffractometer and measured as before, but on air only.

For measurement of wide angle pattern of the packing of the alkyl chains, small portions of dried samples were placed into glass capillaries (diameter 1 mm) and hydrated for at least 36 h in a desiccator at 100% relative humidity. Capillaries were sealed and placed in the X-ray beam of an open pinhole camera operated with Ni-filtered Cu K_α radiation at 30 mA/40 kV. Scattered intensity was collected by a linear position sensitive detector (MBraun, Munich, Germany).

Table 1
Molar mass and fatty acid composition of cardiolipin of *S. aureus* (A); and cardiolipin (B) and lysylcardiolipin (C) from *L. welshimeri* [21,23,28]

Lipid	Mass[a] (Da)	Fatty acid (mol%)[b]															n[c]
		12:0	14i	14.0	15i	15ai	15:0	16i	16:0	17i	17ai	17:0	18:0	18:1	19:0	20:0	20:1	
A	1404	–	3.1	11.7	4.0	11.9	2.5	1.3	15.6	0.7	1.3	1.4	11.6	1.1	4.3	28.7	0.8	16.9
B	1352	1.2	–	1.6	11.4	54.2	–	2.0	3.4	4.2	22.6	–	0.5	–	–	–	–	14.8
C	1480	1.1	–	2.6	10.2	48.9	–	2.1	7.3	3.8	21.3	–	2.5	–	–	–	–	14.7

[a]Molar mass of the free acid form of the predominant molecular species [24].
[b]Abbreviation of fatty acids: e.g. 15i, iso-branched C_{15} (13-methyl-tetradecanoic acid); 15ai, anteiso-branched C_{15} (12-methyl-tetradecanoic acid); for 18:0, 18:1, etc., see Table 2.
[c]n, Average chain length of fatty acids (number of carbon atoms of unbranched chains).

2.5. Sorption measurements

The amount of water sorbed by the cardiolipins investigated was measured gravimetrically with a microbalance system (Sartorius, Göttingen, Germany) between 0 and 100% relative humidity at 25°C. Powdered samples were dried in a stream of dry nitrogen and then subsequently rehydrated by blowing nitrogen gas of definite humidity through the weight cell [26,27].

3. Results and discussion

3.1. Lipids, fatty acid composition and molecular species

The structures of α-D-glucopyranosylcardiolipin and L-lysylcardiolipin are depicted in Fig. 1. Structural analyses, including the cardiolipin from the same bacteria, have been described in detail [19,21–23]. In Tables 1 and 2, the fatty acid compositions are listed. They represent three patterns characteristic of Gram-positive bacteria: (1) straight-chain saturated fatty acids and smaller amounts of iso- and anteiso-branched fatty acids in *S. aureus* [23,28]; (2) more than 90% iso- and anteiso-branched fatty acids in *Listeria* [21]; and (3) straight-chain fatty acids, saturated and *cis*-monounsaturated in *Streptococcus* B [19,22]. The average chain length of *Listeria* fatty acids is by two C-atoms shorter than in *S. aureus* and group B *Streptococcus* lipids. As shown in Fig. 2, in the lipids of group B *Streptococcus* short-chain and unsaturated fatty acids are mostly linked to position 2 of the glycerol moieties. In *S. aureus* [23,28] and *Listeria* lipids [29], the shorter-chain species also occupy predominantly position 2. This distribution pattern is noteworthy because the *sn*-2-fatty acids extend parallel to the plane of the bilayer for their first two carbon atoms and from the third carbon into the bilayer, whereas the *sn*-1-fatty acids extend into the bilayer in full length. In this way, the difference in chain length on the two positions of the glycerol moieties is exaggerated and thus the interdigitation in the methylgroup region enhanced.

Since cardiolipin contains four fatty acids per molecule, a number of fatty acid combinations are possible. The combinations can be elucidated by positive or negative ion FAB MS [24]. In *Listeria* cardiolipin

Table 2
Molar mass and fatty acid composition of cardiolipin and glucosylcardiolipin from *Streptococcus* group B

Lipid	Mass[a] (Da)	Fatty acid (mol%)[b]								n[c]
		12:0	14:0	14:1	16:0	16:1	18:0	18:1	19cy	
Cardiolipin	1404	2.0	3.6	0.6	32.7	14.0	17.4	26.3	3.2	16.8
Glc-cardiolipin	1566	0.9	3.8	1.0	32.8	16.4	16.4	25.2	3.2	16.7

[a]Molar mass of the free acid form of the predominant molecular species (Table 3).
[b]Abbreviation of fatty acids: 18:0, octadecanoic acid; 18:1, Δ11-*cis*-octadecenoic acid; 19cy, *cis*-11,12-methylenoctadecanoic acid.
[c]n, Average chain length of fatty acids (number of carbon atoms).

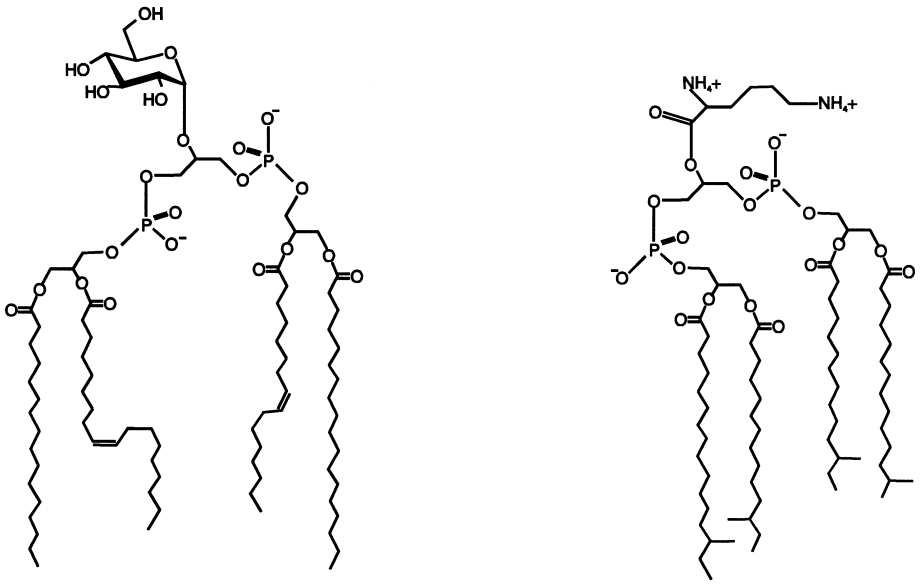

Fig. 1. Structure of α-D-glucopyranosylcardiolipin of *Streptococcus* B and L-lysylcardiolipin of *L. welshimeri*

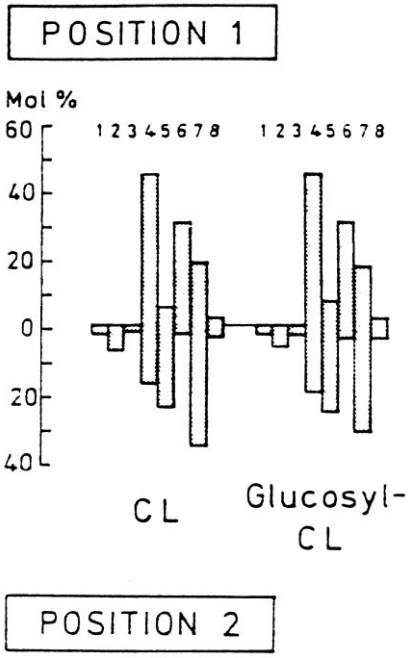

Fig. 2. Distribution of the constituent fatty acids of *Streptococcus* B cardiolipin and glucosylcardiolipin between the two positions of the glycerol moieties [22]. Fatty acids (1–8): 12:0, 14:0, 14:1, 16:0, 16:1, 18:0, 18:1, 19cy (for abbreviations of fatty acids, see Tables 1 and 2).

and lysylcardiolipin ([24] and G. Pohlentz and W. Fischer, unpublished data) seven molecular species of different fatty acid combinations were identified, whereby iso- and anteiso-fatty acids were not discriminated. As shown in Table 3, cardiolipin and glucosylcardiolipin of *Streptococcus* B displayed, respectively, 17 and 14 fatty acid combinations.

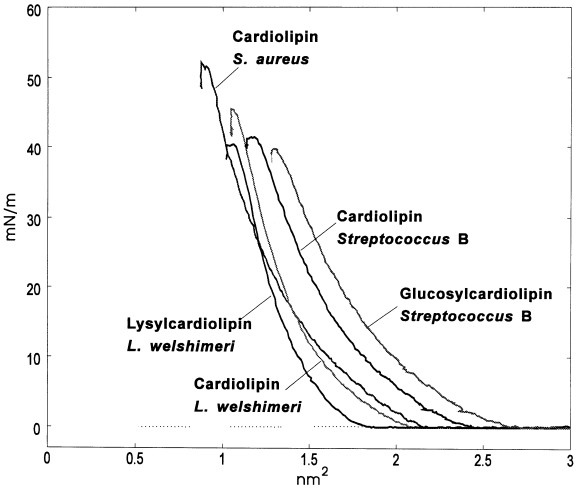

Fig. 3. Isotherms of monofilms of the compounds indicated on the figure. For experimental details see text.

Table 3
Molecular ions in negative ion FAB MS of group B *Streptococcus* cardiolipin and glucosyl cardiolipin

Fatty acid combination	Cardiolipin			Glucosylcardiolipin		
	Mass (Da)	$[M\text{-}H^+]^-$ *m/z*	$[M\text{-}2H^+ + Na^+]^-$ *m/z*	Mass (Da)	$[M\text{-}H^+]^-$ *m/z*	$[M\text{-}2H^+ + Na^+]^-$ *m/z*
18/18/18/18 Δ1	1462	n.d.	1483	1624	n.d.	n.d.
18/18/18/18 Δ2	1460	n.d.	n.d.	1622	1621	1643
19/18/18/16 Δ1	1446	n.d.	1467	1608	n.d.	1629
18/18/18/16 Δ2	1432	1431	1453	1594	1593	1615
18/18/18/16 Δ3	1430	n.d.	1451	1592	n.d.	n.d.
19/18/16/16 Δ1	1418	1417	1439	1580	n.d.	n.d.
18/18/16/16 Δ2	1404	1403**	1425**	1566	1565**	1587*
18/18/16/16 Δ3	1402	n.d.	1423	1564	1563	1585
19/16/16/16 Δ1	1390	n.d.	1411	1552	n.d.	n.d.
18/16/16/16 Δ2	1376	1375*	1397*	1538	1537*	1559**
18/16/16/16 Δ3	1374	n.d.	1395	1536	1535	1557
16/16/16/16 Δ1	1350	1349	1371	1512	1511	n.d.
16/16/16/16 Δ2	1348	1347	1369	1510	1509	1531
16/16/16/16 Δ3	1346	1345	1367	1508	n.d.	n.d.
16/16/16/14 Δ1	1322	1321	1343	1484	1483	1505
16/16/16/14 Δ2	1320	n.d.	1341	1482	1481	1503
16/16/16/14 Δ3	1318	n.d.	1339	1480	n.d.	n.d.
16/16/14/14	1296	n.d.	1317	1458	n.d.	1479
16/16/14/14 Δ1	1294	n.d.	1315	1456	1455	1477
16/16/14/14 Δ2	1292	n.d.	1313	1454	1453	1475
16/16/14/14 Δ3	1290	n.d.	n.d.	1452	1451	1473

Fatty acids are given by their numbers of carbon atoms; 19 stands for 11,12-*cis*-methylenoctodecanoic acid. Δ denotes the number of *cis*-monoenic acids; their assignment to C_{18} or C_{16} would be arbitrary. The most and the next abundant species are marked by two and one asterisk, respectively. In the species 1296–1292 and 1458–1454, the combination 16/14 may be replaced by 18/12. n.d., not detected.

Noteworthy are molecular species that contain three unsaturated fatty acids and, consistent with this observation, species with two unsaturated fatty acids among the phosphatidyl fragments were found (Table 4).

Table 4
Fatty acid composition of phosphatidyl ions formed from glucosylcardiolipin on negative ion FAB MS

m/z	Fatty acids	*m/z*	Fatty acids
715	19/18	659	19/14
713	19/18 Δ1	657	19/14 Δ1
701	18/18 Δ1	645*	18/14 Δ1, 16/16 Δ1
699	18/18 Δ2	643	18/14 Δ2, 16/16 Δ2
687	19/16	631	19/12
685	19/16 Δ1	629	19/12 Δ1
673**	18/16 Δ1**	619	18/12, 16/14
671	18/16 Δ2	617	18/12 Δ1, 16/14 Δ1

For fatty acids, Δ, and asterisks, see Table 3.

3.2. Monofilm measurements

As shown in Fig. 3, the three cardiolipin preparations and the lysyl and glucosyl derivatives formed stable monolayers up to collapse pressures between 40 and 50 mN/m. In contrast to the isotherms of synthetic phospholipids carrying single saturated fatty acid species [30,31], in our experiments, no distinct phase transition was observed. This is characteristic for natural lipid isolates, in which the various molecular species apparently merge into a continuous phase transition.

If one compares the minimal molecular areas of the three cardiolipin preparations (Table 5), one may conclude that their size is determined by the fatty acid composition (Tables 1 and 2). Measuring 1.02 nm^2, it is smallest for *S. aureus* cardiolipin which contains 76% saturated straight-chain and 24% branched fatty acids. An increase to 1.13 nm^2 was found for *L. welshimeri* cardiolipin containing more than 90% saturated iso- and anteiso-branched

fatty acids, and the highest space requirement was observed for *Streptococcus* B cardiolipin in which 45% of the straight-chain fatty acids are *cis*-monounsaturated. Obviously, *cis*-monounsaturated alkyl chains require more space than branched alkyl chains (Fig. 1). The double bonds, which are located near the middle of the chain, cause by a kink in the conformation a less dense packing of the alkyl chains. By contrast, the methyl branches are located near the ω-end of the chain and disturb the alkyl chain packing less.

As shown in Tables 1 and 2, L-lysylcardiolipin and D-glucopyranosylcardiolipin have an almost identical fatty acid composition as the cardiolipin from the same bacterium. The reduced molecular area of lysylcardiolipin therefore suggests that the two-fold positively charged lysyl-residue exerts a condensing effect by charge compensation, whereby it is not yet clear whether one or both amino groups of the lysine moiety are involved. The bulky glucosyl residue increases the space requirement of the headgroup by its size and possibly also by causing a tilt of the fatty acids towards the air–water interface.

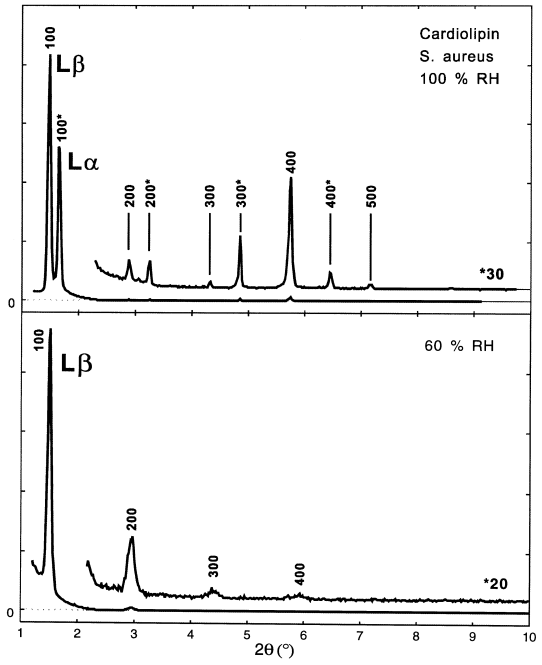

Fig. 4. X-ray powder diffractogram of cardiolipin of *S. aureus*, Na-salt form, at 100% (top) and at 60% (bottom) relative humidity. Orders of Bragg reflections are indicated by the figures. *30, *20 are enlargement factors.

3.3. Small angle X-ray diffraction

The X-ray powder diffraction patterns of bacterial cardiolipins and their derivatives in the sodium salt form are shown in Figs. 4–6. The repeat distances (*d*) derived from X-ray diffraction are listed in Table 6 and will be discussed below along with the bilayer and water layer thickness.

Recorded at 100% relative humidity, the small angle diffraction patterns of all lipids indicated lamellar structures. A high degree of lamellar order can be deduced from the halfwidth between 0.06 and 0.08° 2θ for the first order reflections.

S. aureus and *Streptococcus* B cardiolipin clearly showed two lamellar periodicities (Figs. 4 and 6), indicating the coexistence of lamellar gel and fluid phase (Lβ,Lα). The Lβ phase was predominating in *S. aureus* cardiolipin, the Lα phase in that of group B *Streptococcus*. The phase assignments were also proven by wide-angle X-ray diffraction as shown below. With *L. welshimeri* cardiolipin only the fluid Lα phase was observed (Figs. 5 and 6). This is also true for most of lysylcardiolipin where a shoulder in the diffracted peaks suggests a minor species in the Lβ phase (Fig. 5). The observed phase separation may have occurred on drying the lipids for analysis due to

Table 5
Molecular areas (nm^2) of the various cardiolipins at increasing lateral pressure, derived from Fig. 1

Lipid	10 mN/m	20 mN/m	40 mN/m
Cardiolipin			
S. aureus	1.63 ± 0.03	1.35 ± 0.02	1.02 ± 0.02
L. welshimeri	1.56 ± 0.02	1.35 ± 0.01	1.13 ± 0.01
Streptococcus B	1.85 ± 0.04	1.56 ± 0.02	1.20 ± 0.05
Lysylcardiolipin	1.42 ± 0.03	1.27 ± 0.03	1.09 ± 0.03
Glc-cardiolipin	1.99 ± 0.05	1.69 ± 0.05	1.34 ± 0.04[a]

[a]Measured at 38 mN/m.

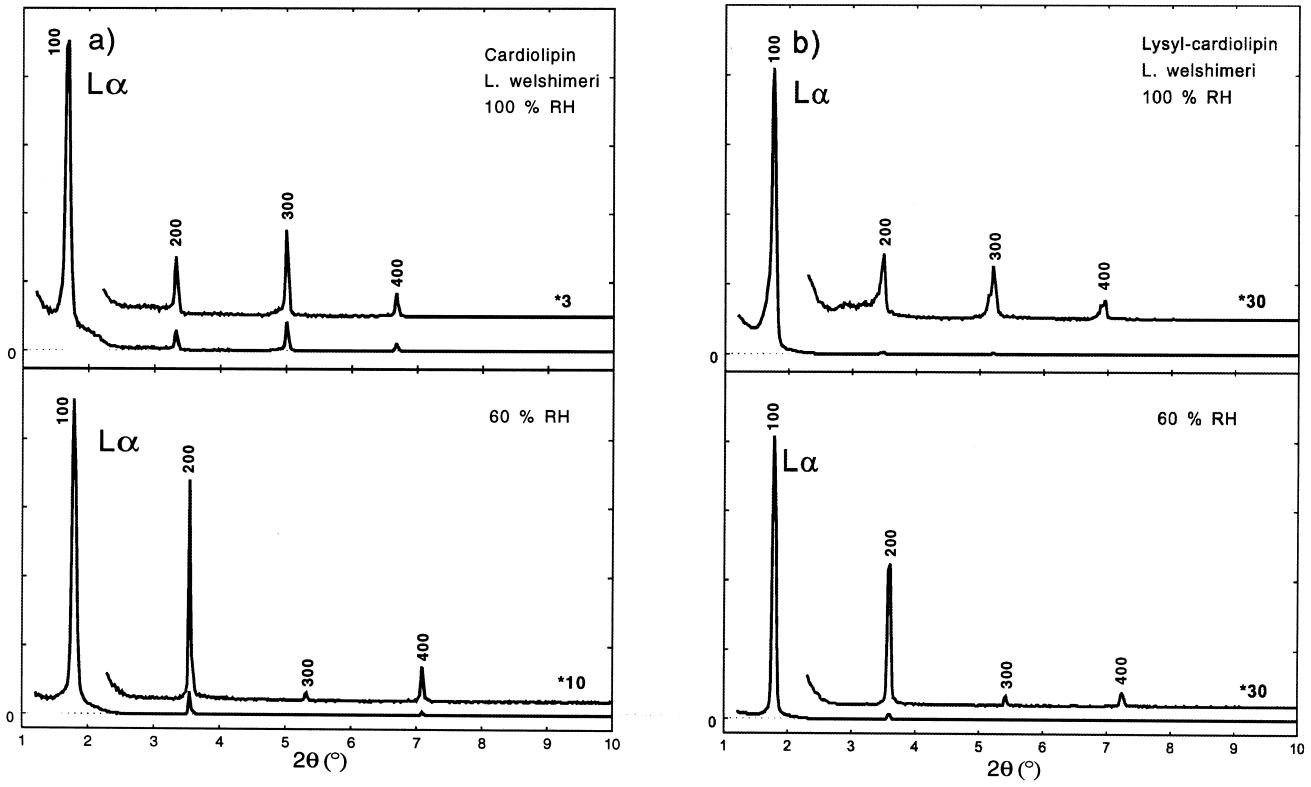

Fig. 5. X-ray powder diffractogram of (a) cardiolipin and (b) lysylcardiolipin of *L. welshimeri*, Na-salt form, at 100% (top) and at 60% (bottom) relative humidity. Orders of Bragg reflections are indicated by the figures. *3, *10 and *30 are enlargement factors.

the presence of molecular species enriched in long chain saturated fatty acids. Noteworthy in this context is the high content of eicosanoate (20:0) in *S. aureus* cardiolipin (Table 1). In the *L. welshimeri* lipids, the less heterogenous fatty acid pattern (Table 1; [24]) may have prevented the formation of two separate phases.

The lower panels in Figs. 4–6 show the diffraction patterns of the sodium salt forms at 60% relative humidity. Under this condition, *S. aureus* and *Streptococcus* B cardiolipin completely changed into the Lβ phase (Figs. 4 and 6), whereas *L. welshimeri* cardiolipin and lysylcardiolipin remained in the fluid state (Fig. 5). The diffraction pattern of glucosylcardiolipin at reduced hydration appears complex (Fig. 6). The pattern fitted best the cubic phase Pn3m [32,33] as shown in Fig. 7. A possible explanation of this deviant behaviour is given below.

When the barium salt forms were analysed at 100% relative humidity, the three lipids tested retained bilayer structures of high order, but completely changed into the lamellar gel phase (Table 6). The barium-induced rigidification of the bilayer was confirmed by wide angle X-ray diffraction (see below).

Fig. 8 depicts the diffractogram of Langmuir–Blodgett multilayer which was prepared from monolayers of *S. aureus* cardiolipin, sodium salt, as described in Section 2. These multilayers also displayed a high degree of lamellar order and showed in addition an exceptionally low layer roughness, as indicated by the well-resolved Kiessig fringes.

3.4. Wide angle X-ray diffraction

Wide angle X-ray diffraction patterns, recorded at 100% relative humidity, are collected in Fig. 9. The peak position was localised by fitting a gaussian curve to the peak profiles. The diffraction pattern of the Na-salt forms show low signal-to-noise ratios. The reflection at $d = 0.441$ nm is characteristic for melted alkyl chains in Lα-phase [32,34,35], the reflection at 0.429 nm is consistent with the Lβ phase which had been identified by small angle X-ray dif-

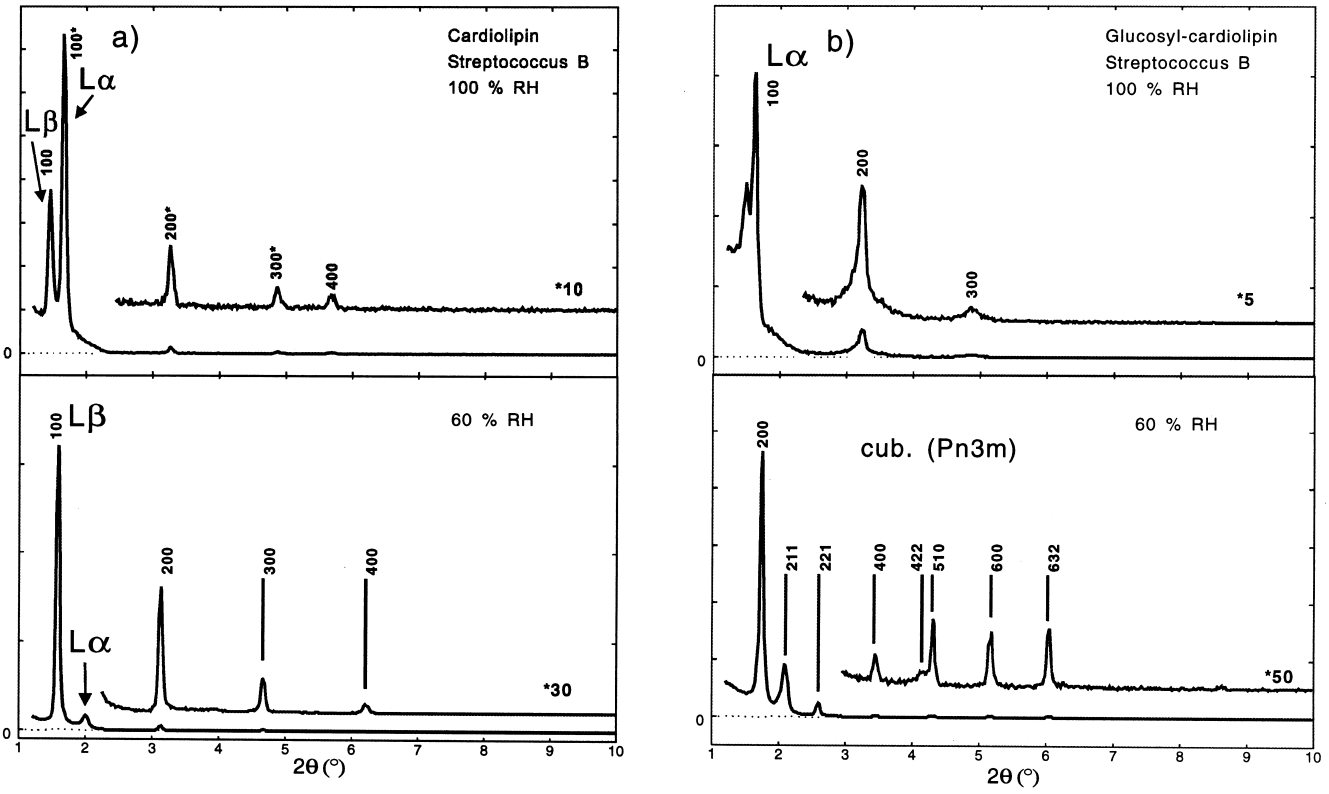

Fig. 6. X-ray powder diffractogram of (a) cardiolipin and (b) glucosylcardiolipin of *Streptococcus* B, Na-salt form, at 100% (top) and at 60% (bottom) relative humidity. Orders of Bragg reflections are indicated by the figures. *5, *10, *30 and *50 are enlargement factors.

fraction in *Streptococcus* B cardiolipin in addition to the Lα phase (Fig. 6).

The barium salt form of *S. aureus* and *Streptococcus* B cardiolipin and glucosylcardiolipin showed reflections between $d = 0.417$ nm and $d = 0.429$ nm corresponding to distances between adjacent alkyl chains from 0.482 to 0.495 nm. These values clearly confirm the Lβ phase [32,34,35] that had been identified by small angle reflections. Under these conditions, the saturated fatty acids of *S. aureus* cardiolipin also packed more tightly and displayed a smaller cross section area than the monounsaturated chains of *Streptococcus* B lipids (Table 7).

3.5. Water sorption

The water sorption was determined as depicted in Fig. 10. The sorption isotherms are similar to those reported earlier [36,37]. $R_{w/l}$ values, taken from the diagrams at 100 and 60% relative humidity, are given in Table 6 and will be discussed below together with the other quantities.

3.6. Bilayer characterisation

Bilayers were characterised by repeat distances (d), surface area per lipid molecule (S), lipid bilayer thickness (d_l), and water layer thickness (d_{H_2O}). The results are listed in Table 6. The equations to calculate these quantities are given in the appendix at the end of the text.

In section Ia of Table 6, the diffraction pattern of the sodium salts were recorded at 100% relative humidity. Under these conditions, the repeat distances of Lα phase cardiolipin bilayers varied between 5.25 and 5.52 nm; the contribution of the water layer to this distance was approximately 25% ($100 \cdot d_{H_2O}/d$). The surface areas were in the range between 1.08 and 1.26 nm^2. For Lα phase of bovine heart cardiolipin, a lipid surface area of 1.42 nm^2 was reported

Table 6
Bilayer characterization

Lipid, salt form	d (nm)	Phase	S (nm^2)	$R_{w/l}$	d_l (nm)	d_{H_2O} (nm)	d_{H_2O}/d
(Ia) Sodium salt, 100% RH							
Cardiolipin							
S. aureus	5.52 ± 0.08	L α	1.11 ± 0.04	} 25.0 ± 0.5	4.20	1.32	0.24
	6.18 ± 0.03	L β	–		–	–	–
L. welshimeri	5.31 ± 0.02	L α	1.08 ± 0.01	20.8 ± 0.4	4.16	1.15	0.22
Streptococcus B	5.25 ± 0.03	L α	1.26 ± 0.04	} 32.8 ± 0.7	3.70	1.55	0.28
	5.92 ± 0.03	L β	–		–	–	–
Lysylcardiolipin	5.12 ± 0.03	L α	1.10 ± 0.02	12.4 ± 0.3	4.46	0.66	0.13
Glc-cardiolipin	4.99 ± 0.20	L α	1.27 ± 0.05	19.2 ± 0.4	4.09	0.90	0.18
(Ib) Sodium salt, 60% RH							
Cardiolipin							
S. aureus	6.18 ± 0.03	L β	0.83 ± 0.05	8.8 ± 0.4	5.61	0.57	0.10
L. welshimeri	4.99 ± 0.03	L α	0.97 ± 0.05	5.8 ± 0.3	4.62	0.37	0.08
Streptococcus B	4.65 ± 0.03	L α[a]	–	} 4.6 ± 0.4	–	–	–
	5.58 ± 0.10	L β	0.88 ± 0.05		5.29	0.29	0.05
Lysylcardiolipin	4.85 ± 0.03	L α	1.04 ± 0.05	2.0 ± 0.3	4.72	0.13	0.03
Glc-cardiolipin	10.15 ± 0.10	cub.	–	4.5 ± 0.4	–	–	–
(II) Barium salt, 100% RH							
Cardiolipin							
S. aureus	5.84 ± 0.03	Lβ	0.88 ± 0.05	8.0 ± 0.4	5.29	0.55	0.09
Streptococcus B	5.57 ± 0.03	Lβ	0.98 ± 0.06	14.0 ± 0.4	4.75	0.82	0.14
Glc-cardiolipin	5.30 ± 0.20	Lβ	1.26 ± 0.05	25.4 ± 0.6	4.13	1.17	0.22

Repeat distances (d), surface area per lipid molecule (S), water molecules sorbed ($R_{w/l}$), lipid bilayer thickness (d_l), and water layer thickness (d_{H_2O}). In mixed phases, $R_{w/l}$ of Lα and Lβ could not be determined separately. Powdered X-ray diffractions and sorbed water were measured at 25°C and 100% (Ia, II), respectively 60% relative humidity (Ib). For molar masses, see Tables 1 and 2.
[a]Minor fraction (see Fig. 6).

[11], but this high value may be ascribed to the content of 70% of the more space-requiring octadidecenoic acid in the mitochondrial cardiolipins. In *Streptococcus* B cardiolipin, the effect of unsaturated fatty acids became apparent in an increased surface area combined with a lower thickness of the lipid layer which, in spite of the slightly increased water layer thickness, led to the smallest repeat distance observed here.

Compared with the unsubstituted counterparts, lysyl and glucosylcardiolipin showed a similar surface area, but, apparently due to the substituent, a larger lipid layer thickness. With both lipids, the amount of sorbed water was significantly reduced and the decreased water layer thickness calculated therefrom appears to be the main reason for the observed diminished repeat distances. The large surface area and the relatively small lipid layer thickness also reflected the presence of unsaturated fatty acids for glucosylcardiolipin.

In the case of lysylcardiolipin, electrostatic interaction between opposite membrane surfaces and possibly the hydrophobic methylene groups of the lysyl residues may contribute to the reduced water-binding capacity. The diminished water-binding by glucosylcardiolipin is less clear and requires further studies. One is tempted to speculate that hydrogen bonds between sugar residues and phosphate groups of opposite bilayer surfaces lead to lower water sorption and diminished repeat distance. In view of the low water sorption, it should also be pointed out that hydrophobic interactions between the axial protons of the pyranose rings of glycolipids have been observed [38].

In section Ib of Table 6, the reduction of the relative humidity to 60% led to two significant changes:

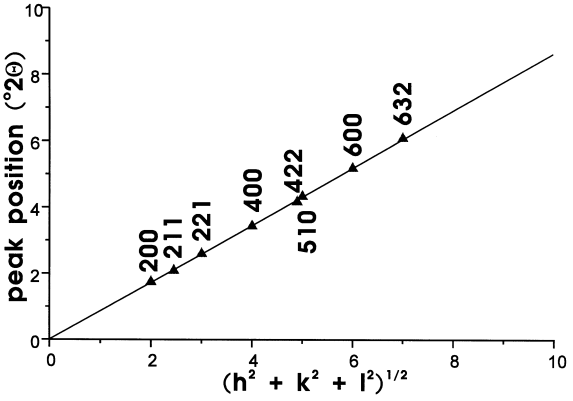

Fig. 7. Scattering angles of diffraction peaks of Fig. 6b (bottom) vs $(h^2+k^2+l^2)^{1/2}$ for the hkl indices of the expected cubic reflections.

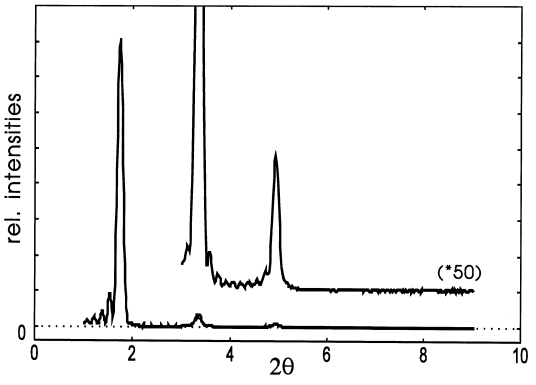

Fig. 8. X-ray powder diffractogram of Langmuir–Blodgett multilayers of cardiolipin of *S. aureus*. *50 is enlargement factor.

the number of the absorbed water molecules was drastically diminished and, as noted above, *S. aureus* and *Streptococcus* B cardiolipin bilayers had virtually completely adopted the lamellar gel phase. The reduced repeat distances in section Ib can be mostly ascribed to the reduced water layer thickness. Compared with the fluid phase in section Ia, the stretched fatty acid conformation in the Lβ phase of *S. aureus* and *Streptococcus* B cardiolipin bilayers is reflected by an increase of the bilayer thickness accompanied by a reduction of the lipid surface area. A slight increase in the bilayer thickness was observed for *L. welshimeri* cardiolipin and lysylcardiolipin, both of which remained under reduced hydration in the lamellar fluid phase.

The arrangement of glucosylcardiolipin in cubic phase was mentioned above. In cubic phases, three-dimensional lattice of inverted micelles or connected inverted rods may form [32,33], which is usually the case when the cross-sectional area of the headgroup is smaller than the cross-sectional area of the hydrophobic moiety. This principle cannot be applied to glucosylcardiolipin without modification. We suggest that under reduced hydration the hydrogen bonds postulated above between sugar residues and phosphate groups of opposite bilayer surfaces may increase in number and/or strength, thus urging the lipid molecules to adopt the inverted supramolecular structure. Inverted non-lamellar hexagonal structures were observed in mixtures of POPC and non-ionic surfactant under similar conditions at reduced hydration [39,40].

In section II of Table 6, Na^+ was replaced as counterion by Ba^{2+}, and X-ray reflections were recorded at 100% relative humidity as in section Ia. The three lipids tested adopted the Lβ phase which in the case of the two cardiolipin preparations was also reflected by a reduced surface area and an increased lipid layer thickness. In both preparations the water layer thickness was drastically reduced, suggesting that the barium phosphate groups are less dissociated than the sodium salt forms. Also here the glucosylcardiolipin behaved differently in

Table 7
Wide angle X-ray diffraction of cardiolipins and glucosylcardiolipin in Ba-salt form

Lipid	d_{waxs} (nm)	a (nm)	S^a_{ch} (nm^2)	φ_{ch} (°)
Cardiolipin				
S. aureus	0.417 ± 0.005	0.482 ± 0.005	0.201 ± 0.004	32.7 ± 1.0
Streptococcus B	0.429 ± 0.006	0.495 ± 0.006	0.212 ± 0.005	47.5 ± 1.0
Glc-cardiolipin	0.424 ± 0.006	0.490 ± 0.006	0.208 ± 0.005	51.6 ± 1.5

d_{waxs}, d-spacing; a, lattice constant, distance between adjacent alkyl chains ($a=[2/\sqrt{3}]\cdot d_{waxs}$); S_{ch}, cross-sections of alkyl chains; φ_{ch}, tilt of alkyl chains.

[a] $S_{ch} = d_{waxs}[2/\sqrt{3}]d_{waxs}$.

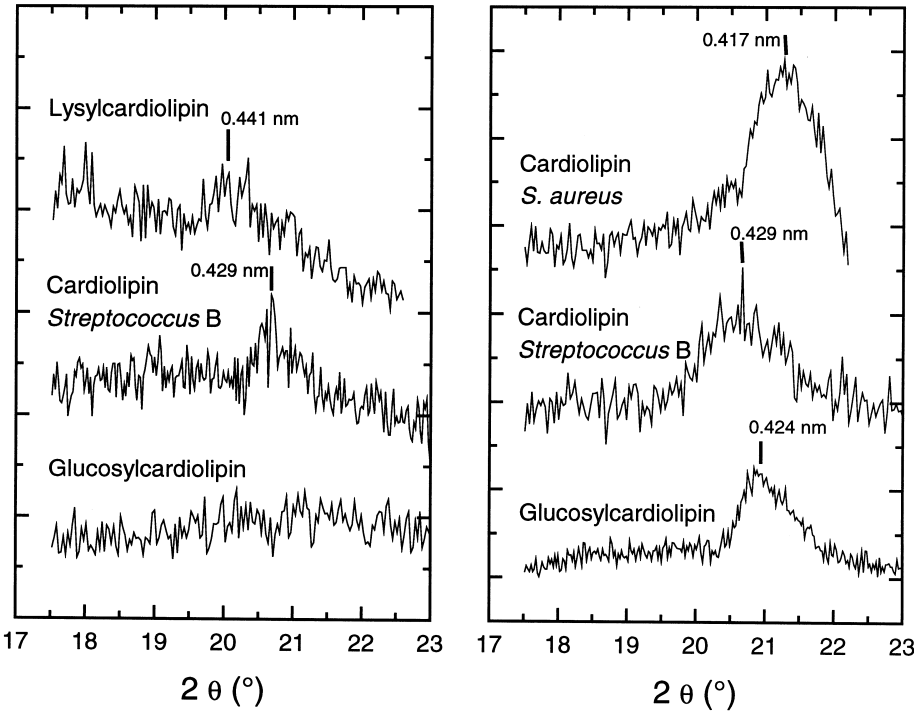

Fig. 9. Wide angle X-ray powder diffraction (100% relative humidity). Na-salt form (left), Ba-salt form (right). For peak location see text.

so far as the sorption of water molecules and the thickness of the water layer exceeded the values measured for he sodium salt form (Table 6, section Ia). An explanation might be that the large barium ions and/or the less dissociated barium phosphate groups prevented the above-postulated formation of hydrogen bonds between opposite bilayer surfaces thus enabling the sugar hydroxyls freely to interact with water.

If one compares the Lβ phase of *S. aureus* and *Streptococcus* B cardiolipin in section Ib with the Lβ phase in section II, it becomes apparent that in section II the lipid layer thickness was significantly reduced. We ascribe this effect to the tilt of fatty acids which, as shown in Table 7, were tilted 33° and 47° away from the bilayer normal. Comparable values have been reported for charged phospholipids DPPG and DHPA [41,42].

The highest tilt was found for the fatty acids in the glucosylcardiolipin bilayer. In this case, a diminished lipid layer thickness becomes evident if one considers that it was in the Lβ phase (section II) practically the same as in the Lα phase (section Ia). Also the surface area remained nearly constant (Table 6).

3.7. Electron density profiles

Electron density profiles were calculated according to [43]

$$\rho(x) = \Sigma \pm a_h \cos(2\pi hx/d)$$

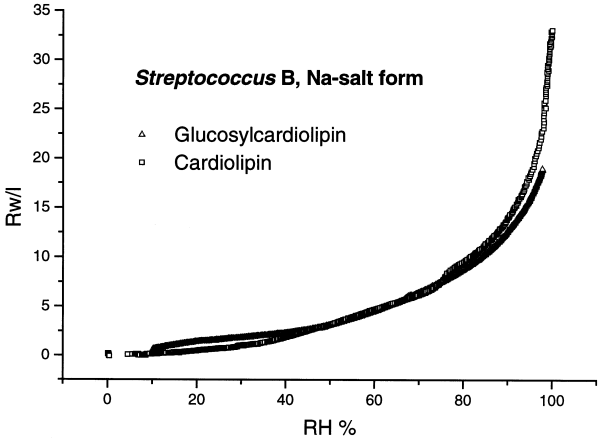

Fig. 10. Sorption isotherm of *Streptococcus* B cardiolipin and glucosylcardiolipin (Na-salt form, 25°C). The relative humidity was in a stream of nitrogen increased continuously over 20.7 h and 31.9 h for cardiolipin and glucosylcardiolipin, respectively. Equipment and procedure according to [26,27].

The amplitudes of the cosine functions are $a_h = \sqrt{(I_h\ h)}$, were h is the order of the observed reflection; I_h is the observed maximum of the intensity of reflection h (Table 8) and d is the repeat distance. The appropriate sign of a_h has been chosen by trial and error of possible electron density functions to fit the Fourier transform of the profile at different hydration states.

The electron density profiles obtained are shown in Fig. 11. The low density trough at 0 nm corresponds to the terminal methyl groups in the geometric centre of the bilayer, the highest density peaks correspond to the lipid headgroups, the medium density regions between the methyl trough and the headgroups correspond to the methylene chains [44,45]. The electron density profiles of *Listeria* cardiolipin and lysylcardiolipin, Na^+ form, show a broad methyl trough and a smooth, more-or-less continuous increase, consistent with fluid hydrocarbon chains (cf. Fig. 5). The location of the phosphate group is not influenced by the lysyl substituent. Located at 1.92 nm above the bilayer centre it differs only slightly from that of cardiolipin at 1.88 nm.

In the electron density profile of the barium salts of *Streptococcus* B cardiolipin and glucosylcardiolipin, the methyl trough was narrower and deeper, the increase two-stepped and steeper (Fig. 11b) consistent with the lamellar gel phase (Table 6). The glucosyl substituent shifted the maximum from 1.80 to

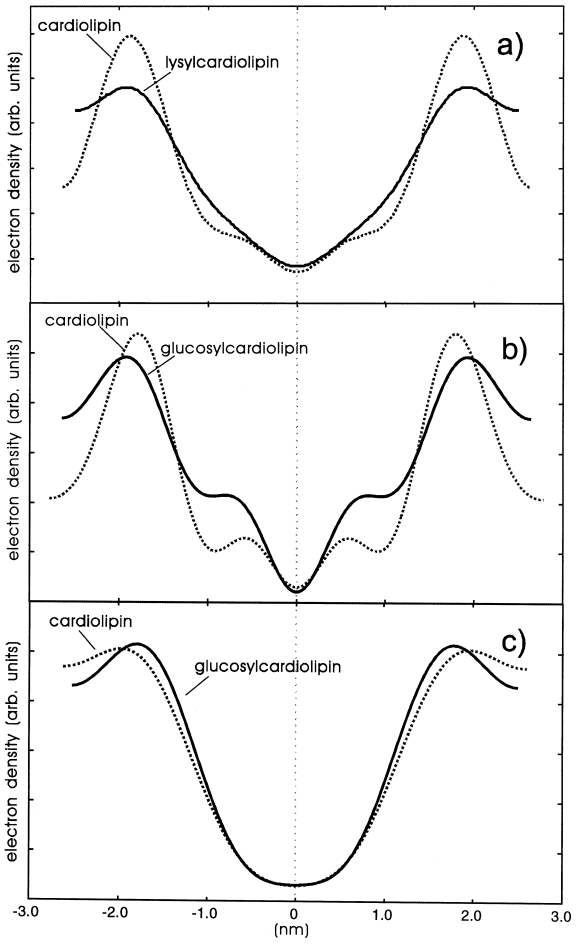

Fig. 11. Electron density profiles of (a) cardiolipin and lysylcardiolipin of *L. welshimeri*, Na-salt form, (b) cardiolipin and glucosylcardiolipin of *Streptococcus* B, Ba-salt form, and (c) Na-salt form at 100% relative humidity, respectively.

Table 8
Measured relative intensities and amplitudes of cosine function a_h of observed orders of diffraction of cardiolipins, Na and Ba-salt form at 100% relative humidity

Lipid	Relative intensity and a_h									
	d (nm)	$h=1$		$h=2$		$h=3$		$h=4$		$h=5$	
		Int.	a_h	Int.	a_h	Int.	a_h	Int.	a_h	Int.	a_h
Sodium salt											
Cardiolipin											
Streptococcus B	5.25	100	−10	1.9	−2.0	0.7	+1.4	–	–	–	–
L. welshimeri	5.31	100	−10	6.4	−3.6	9.4	+5.3	2.5	−3.2	–	–
Lysylcardiolipin	5.12	100	−10	0.7	−1.2	0.6	+1.3	0.2	−0.9	–	–
Glc-cardiolipin	4.99	100	−10	9.6	−4.4	1.0	+1.7	–	–	–	–
Barium salt											
Cardiolipin											
Streptococcus B	5.25	100	−10	22.9	−6.7	17.9	+7.3	0.8	−1.8	2.4	−3.4
Glc-cardiolipin	4.99	100	−10	2.8	−2.3	0.7	+3.3	2.1	−2.9	–	–

1.98 nm. The electron density profiles of the sodium salts of these two lipids are depicted in Fig. 11c. The profiles along the hydrocarbon chains are consistent with the fluid state (cf. Fig. 6). Whereas the headgroup of cardiolipin was located at 1.98 nm above the bilayer centre, that of the glucosyl derivative was with 1.68 nm drastically reduced. We have no explanation for this deviant behaviour. We believe, however, that it signalises an unusual orientation of the glucosyl substituted headgroup which might play a role in the reduced hydration and the diminished repeat distance reported above.

4. Conclusions

The three cardiolipin preparations as well as the lysyl- and glucosyl-derivative isolated from Gram-positive bacteria displayed different fatty acid patterns and were composed of numerous species differing in fatty acid combinations. In spite of these heterogeneities, all lipids investigated formed stable monolayers and spontaneously adopted bilayer structures of a high degree of order. The fatty acid mixtures of the individual lipids are responsible for the continuous fluid-to-gel phase transition in the monofilm experiments and in some cases the observed coexistence of lamellar gel and fluid phase. The surface areas of the cardiolipin preparations, determined in the monolayer experiment near the collapse pressure and measured in the bilayer structures at 100% relative humidity, showed a fairly good agreement and were essentially determined by the fatty acid composition. It is noteworthy that for bilayer arrangements a lateral pressure of 30–35 mN/m has been reported [46].

In the monolayer experiment, the lysyl substituent exerted a condensing effect, whereas the glucosyl substituent led to an increase of the surface area. These effects were not seen in the bilayer structures. Instead, both substituents caused a decreased water sorption per lipid molecule and a diminished repeat distance. These observations prompted us to hypothesise electrostatic interactions, respectively, hydrogen bonds between opposing bilayer surfaces. Other deviant properties of glucosylcardiolipin, namely a cubic phase supramolecular structure under reduced hydration, and an increased instead of a decreased water sorption in the barium salt form, require further experiments.

Acknowledgements

W.F. thanks Morris Kates for stimulating discussions, Edeltraut Ebnet and Barbara Orlicz-Welcz for their help in isolation and characterisation of the lipids. The financial support by the Deutsche Forschungsgemeinschaft is gratefully acknowledged (Br-321/31-1, Fi-218/7-1). The FAB MS analyses were supported by EC Training and Mobility of Researchers-Access to Large-Scale Facilities, EC/CNR Contract ERB FMGECT95 0061. Mass spectral data were provided by the European Mass Spectrometry Facility Centre, CNR-Napoli (Italy). The skilful assistance of Dr. Gabriella Pocsfalvi is gratefully acknowledged.

Appendix

The following equations were used to calculate the quantities given in Table 6. This Table also contains the figures required for calculations.

The surface area per molecule [33,47] was calculated by:

$$S = 2(V_l + R_{w/l} \cdot V_w)/d$$

where V_l is the volume of one lipid molecule (nm^3), calculated by dividing the molecular mass (Tables 1 and 2) by the density of the lipid (1 g/cm^3) and 6.023×10^{23} (Avogadro number), R_w/l is the number of water molecules sorbed by one lipid molecule, V_w, volume of one water molecule (0.030 nm^3) and d is the repeat distance.

The thickness of the water layer between opposing hydrophilic headgroups, assuming total separation of lipid and water volume [33,43] was calculated by:

$$d_{H_2O} = 2(R_{w/l} \cdot V_w)/S$$

The thickness of the lipid bilayer [33,48] was determined by:

$$d_l = 2V_l/S$$

The tilt angles (φ°_{ch}) of the alkyl chains in Table 7 were calculated as follows [41,49]:

$$\varphi^{\circ}_{ch} = \cos^{-1}(nS_{ch}/S)$$

where $n = 4$ is the number of alkyl chains and S_{ch} is the cross-sectional area per alkyl chain (Table 7).

References

[1] G. Daum, Lipids of mitochondria, Biochim. Biophys. Acta 822 (1985) 1–42.

[2] L.F. Hoch, Cardiolipins and biomembrane function, Biochim. Biophys. Acta 1113 (1992) 71–133.

[3] W.M. O'Leary, S.G. Wilkinson, Gram positive bacteria, in: C. Ratledge, S.G. Wilkinson (Eds.), Microbial Lipids, Vol. 1, Academic Press, New York, 1988, pp. 117–200.

[4] Wilkinson, S.G., Gram negative bacteria, in: C. Ratledge, S.G. Wilkinson (Eds.), Microbial Lipids, Vol. 1, Academic Press, New York, 1988, pp. 299–488.

[5] H.U. Koch, R. Haas, W. Fischer, The role of lipoteichoic acid biosynthesis in membrane lipid metabolism of growing *Staphylococcus aureus*, Eur. J. Biochem. 138 (1984) 357–363.

[6] S.A. Short, D.C. White, Metabolism of phosphatidylglycerol, lysylphosphatidyl-glycerol and cardiolipin of *Staphylococcus aureus*, J. Bacteriol. 108 (1971) 219–226.

[7] Y. Kanemasa, T. Yioshioka, H. Hayashi, Alteration of the phospholipid composition of *Staphylococcus aureus* cultures in medium containing NaCl, Biochim. Biophys. Acta 280 (1972) 444–450.

[8] A. Okabe, Y. Hirai, H. Hayashi, Y. Kanemasa, Alteration in phospholipid composition of *Staphylococcus aureus* during formation of autoplast, Biochim. Biophys. Acta 617 (1980) 28–35.

[9] P.R. Allegrini, G. Pluschke, J. Seelig, Cardiolipin conformation and dynamics in bilayer membranes as seen by deuterium magnetic resonance, Biochemistry 23 (1984) 6452–6458.

[10] P.R. Cullis, A.J. Verkleij, P.H.J.Th. Ververgart, Polymorphic phase behaviour of cardiolipin as detected by ^{31}P NMR and freeze-fracture techniques. Effects of calcium, dibucaine and chlorpromazine, Biochim. Biophys. Acta 513 (1978) 11–20.

[11] J.M. Seddon, R.D. Kaye, D. Marsh, Induction of the lamellar-inverted hexagonal phase transition in cardiolipin by protons and monovalent cations, Biochim. Biophys. Acta 734 (1983) 347–352.

[12] G.L. Powell, D. Marsh, Polymorphic phase behaviour of cardiolipin derivatives studied by ^{31}P NMR and X-ray diffraction, Biochemistry 24 (1985) 2902–2908.

[13] W. Hübner, H.H. Mantsch, M. Kates, Intramolecular hydrogen bonding in cardiolipin, Biochim. Biophys. Acta 1066 (1991) 166–174.

[14] M. Kates, J.-Y. Syz, D. Gosser, T.H. Haines, pH-Dissociation characteristics of cardiolipin and its 2′-deoxy analogue, Lipids 28 (1993) 877–882.

[15] J. Teissié, M. Prats, P. Soucaille, J.F. Tocanne, Evidence for conduction of protons along the interphase between water and a polar lipid monolayer, Proc. Natl. Acad. Sci. USA 82 (1985) 3217–3221.

[16] J. Heberle, J. Riesle, G. Thiedemann, D. Oesterhelt, N.A. Dencher, Proton migration along the membrane surface and retarded surface to bulk transfer, Nature 370 (1994) 379–382.

[17] P. Scherrer, U. Alexiev, T. Marti, H.G. Khorana, M.P. Heyn, Covalently bound pH-indicator dyes at selected extracellular or cytoplasmic sites in bacteriorhodopsin. 1. Proton migration along the surface of bacteriorhodopsin micelles and its delayed transfer from surface to bulk, Biochemistry 33 (1994) 13684–13692.

[18] P. Scherrer, Proton movement on membranes, Nature 374 (1995) 222.

[19] W. Fischer, The polar lipids of group B streptococci. I. Glucosylated diphosphatidyl-glycerol, a novel glycophospholipid, Biochim. Biophys. Acta 487 (1977) 74–88.

[20] W. Fischer, D. Arneth-Seifert, D-Alanylcardiolipin, a major component of the unique lipid pattern of *Vagococcus fluvialis*, J. Bacteriol. 180 (1998) 2950–2957.

[21] W. Fischer, K. Leopold, The polar lipids of four listeria species containing L-lysylcardiolipin, a novel lipid structure, Int. J. System. Bact. 49 (1999) 653–662.

[22] W. Fischer, The polar lipids of group B streptococci. II. Composition and positional distribution of fatty acids, Biochim. Biophys. Acta 487 (1977) 89–104.

[23] W. Fischer, Lipoteichoic acids and lipids in the membrane of *Staphylococcus aureu*, Med. Microbiol. Immunol. 183 (1994) 61–76.

[24] J. Peter-Katalinic', W. Fischer, α-D-Glucopyranosyl, D-alanyl, and L-lysyl-cardiolipin from gram-positive bacteria. Analysis by fast atom bombardment mass spectrometry, J. Lipid Res. 39 (1998) 2286–2292.

[25] P. Fromherz, Instrumentation for handling monomolecular films at an air–water interface, Rev. Sci. Instrum. 46 (1975) 1380–1385.

[26] H. Binder, B. Kohlstrunk, H.H. Heerklotz, A humidity titration calorimetry technique to study the thermodynamics of hydration, Chem. Phys. Lett. 304 (1999) 329–335.

[27] H. Binder, A. Anikin, B. Kohlstrunk, G. Klose, Hydration induced gel states of the dienic lipid 1,2-bis(2,4-octadecanoyl)-sn-glycero-3-phosphorylcholine and their characterization using infrared spectroscopy, J. Phys. Chem. B 101 (1997) 6618–6628.

[28] T. Gutberlet, J. Frank, H. Bradaczek, W. Fischer, Effect of lipoteichoic acid on thermotropic membrane properties, J. Bacteriol. 179 (1997) 2879–2883.

[29] N. Kosaric, K.K. Caroll, Phospholipids of *Listeria monocytogenes*, Biochim. Biophys. Acta 239 (1971) 428–442.

[30] G.L. Gaines Jr., Insoluble Monolayers at Liquid–Gas Interfaces, Interscience, New York, 1966.

[31] A.W. Adamson, Physical Chemistry of Surfaces, Wiley-Interscience, New York, 1990.
[32] V. Luzzati, X-ray diffraction studies of lipid–water systems, in: D. Chapman (Ed.), Biological Membranes – Physical Fact and Function, Academic Press, London, 1968, pp. 71–123.
[33] P. Mariani, V. Luzzati, H. Delacroix, Cubic phases of lipid-containing systems – structure analysis and biological implications, J. Mol. Biol. 204 (1988) 165–189.
[34] M.J. Janiak, D.M. Small, G.G. Shipley, Nature of the thermal pretransition of synthetic phospholipid: dimyristoyl- and dipalmitoyllecithin, Biochemistry 15 (1976) 4575–4580.
[35] S.M. Gruner, M.K. Jain, X-ray diffraction demonstrates that phosphatidyldiacylglycerol and phosphatidylcholesterol are not lamellar above the main transition temperature, Biochim. Biophys. Acta 818 (1985) 352–355.
[36] G. Klose, B. König, F. Paltauf, Sorption isotherms and swelling of POPC in H_2O and ^2H_2O, Chem. Phys. Lipids 61 (1992) 265–270.
[37] B.W. Koenig, H.H. Stey, K. Gawrisch, Membrane lateral compressibility determined by NMR and X-ray diffraction: effect of acyl chain polyunsaturation, Biophys. J. 73 (1997) 1954–1966.
[38] A. Geyer, C. Gege, R.R. Schmidt, Carbohydrate–carbohydrate recognition between $Lewis^X$ glycoconjugates, Angew. Chem. Int. Ed. 38 (1999) 1466–1468.
[39] B. König, U. Dietrich, G. Klose, Hydration and structural properties of mixed lipid/surfactant model membranes, Langmuir 13 (1997) 525–532.
[40] G. Klose, S. Eisenblätter, B. König, Ternary phase diagram of mixtures of palmitoyl-oleyl-phosphatidylcholine, tetraoxyethylene dodecyl ether, and heavy water as seen by ^{31}P and ^2H NMR, J. Colloid Interface Sci. 172 (1995) 438–446.
[41] F. Jähnig, K. Harlos, H. Vogel, H. Eibl, Electrostatic interactions at charged lipid membranes. Electrostatically induced tilt, Biochemistry 18 (1979) 1459–1467.
[42] A. Watts, K. Harlos, D. Marsh, Charge-induced tilt in ordered-phase phosphatidylglycerol bilayers evidence from X-ray diffraction, Biochim. Biophys. Acta 645 (1981) 91–96.
[43] N.P. Franks, W.R. Lieb, X-ray and neutron diffraction studies of lipids bilayers, in: C.G. Knight (Ed.), Liposomes: From Physical Structure to Therapeutic Applications, Elsevier North Holland, Amsterdam, 1981, pp. 243–272.
[44] T.J. McIntosh, A.D. Magid, S.A. Simon, Steric repulsion between phosphatidylcholine bilayers, Biochemistry 26 (1987) 7325–7332.
[45] T.J. McIntosh, S.A. Simon, Contributions of hydration and steric (entropic) pressures to the interactions between phosphatidylcholine bilayers: experiments with the subgel phase, Biochemistry 32 (1993) 8374–8384.
[46] D. Marsh, Lateral pressure in membranes, Biochim. Biophys. Acta 1286 (1996) 183–223.
[47] J.M. Seddon, Structure of the inverted hexagonal (H_{II}) phase, and non-lamellar phase transitions of lipids, Biochim. Biophys. Acta 1031 (1990) 1–69.
[48] G. Cevc, D. Marsh, Phospholipid Bilayers – Physical Principles and Models, J. Wiley and Sons, New York, 1987.
[49] J.M. Seddon, G. Cevc, R.D. Kaye, D. Marsh, X-ray diffraction study of the polymorphism of hydrated diacyl- and dialkylphosphatidylethanolamines, Biochemistry 23 (1984) 2634–2644.